

# Hydraulic Turbines

# 9

*Hear ye not the hum of mighty workings?*

*John Keats, Sonnet No. 14*

*The power of water has changed more in this world than emperors or kings.*

**Leonardo da Vinci**

## 9.1 INTRODUCTION

To put this chapter into perspective some idea of the scale of hydropower development in the world might be useful before delving into the intricacies of hydraulic turbines. A very detailed and authoritative account of virtually every aspect of hydropower is given by Raabe (1985) and this brief introduction serves merely to illustrate a few aspects of a very extensive subject.

Hydropower is the longest established source for the generation of electric power, which, starting in 1880 as a small dc generating plant in Wisconsin, United States, developed into an industrial size plant following the demonstration of the economic transmission of high voltage ac at the Frankfurt Exhibition in 1891. Hydropower was expected to have a worldwide yearly growth rate of about 5% (i.e., doubling in size every 15 years) but this rate has now proved to be too optimistic. In 1980 the worldwide installed generating capacity was 460 GW according to the United Nations (1981) but in 2007 the figure was just exceeding 700 GW. This works out at roughly 1.6% annual yearly growth. The smaller growth rate must, primarily, be due to the high costs involved in the civil engineering work, the cost of the power and related electrical plant, and to some extent the human cost due to massive population displacements with necessary new building.

According to the Environmental Resources Group Ltd., in 2007 hydropower constituted about 21% of the world's electrical generating capacity. The theoretical potential of hydropower is believed to be 2800 GW. The main areas with potential for growth are China, Latin America, and Africa.

Table 9.1 is an extract of data quoted by Raabe (1985) of the distribution of harnessed and harnessable potential of some of the countries with the biggest usable potential of hydropower. From this list it is seen that the People's Republic of China (PRC), the country with the largest harnessable potential in the world had, in 1974, harnessed only 4.22% of this. However, the Three Gorges Dam project on the Yangtse River, is now the biggest hydropower plant in the world. It contains 32 Francis turbines

**Table 9.1** Distribution of Harnessed and Harnessable Potential of Hydroelectric Power

Country	Usable Potential, TWh	Amount of Potential Used, TWh	Percentage of Usable Potential
1 China (PRC)	1320	55.6	4.22
2 Former USSR	1095	180	16.45
3 USA	701.5	277.7	39.6
4 Zaire	660	4.3	0.65
5 Canada	535.2	251	46.9
6 Brazil	519.3	126.9	24.45
7 Malaysia	320	1.25	0.39
8 Columbia	300	13.8	4.6
9 India	280	46.87	16.7
Sum 1–9	5731	907.4	15.83
Other countries	4071	843	20.7
Total	9802.4	1750.5	17.8

each capable of generating 700 MW, and in 2011, when all of the plant is fully operational, the total generating capacity will be 22,500 MW.

### Tidal Power

This relatively new and very promising technology, in which tidal stream generators are used to generate power, is still under active development. Very large amounts of energy can be obtained by this means and, unlike wind power and solar power, it is available at known times each day. The most efficient type of generator is still to be determined. The world's first commercial tidal stream generator, *SeaGen*, was installed in 2008 at Strangford Lough, Northern Ireland. The prototype version comprises two 600 kW axial-flow turbines, 16 m in diameter. Further details on this tidal turbine are given towards the end of this chapter.

### Wave Power

Several energy conversion systems have now been developed for obtaining electrical power from sea waves. One notable example is the *Wells turbine*, which uses an oscillating water column generated by the waves to drive this special type of axial-flow turbine. Several of these turbines have been installed (in Scotland and India) and details of their rather special fluid mechanical design are given in this chapter.

### Features of Hydropower Plants

The initial cost of hydropower plants may be much higher than those of thermal power plants. However, the present value of total costs (which includes those of fuel) is, in general, lower in hydropower plants. Raabe (1985) listed the various advantages and disadvantages of hydropower plants and a brief summary of these is given in Table 9.2.

**Table 9.2** Features of Hydroelectric Power Plants

Advantages	Disadvantages
<p>Technology is relatively simple and proven. High efficiency. Long useful life. No thermal phenomena apart from those in bearings and generator.</p> <p>Small operating, maintenance, and replacement costs.</p> <p>No air pollution. No thermal pollution of water.</p>	<p>Number of favourable sites limited and available only in some countries. Problems with cavitation and water hammer.</p> <p>High initial cost especially for low head plants compared with thermal power plants.</p> <p>Inundation of the reservoirs and displacement of the population. Loss of arable land. Facilitates sedimentation upstream and erosion downstream of a barrage.</p>

## 9.2 HYDRAULIC TURBINES

### Early History of Hydraulic Turbines

The hydraulic turbine has a long period of development, its oldest and simplest form being the waterwheel, first used in ancient Greece and subsequently adopted throughout medieval Europe for the grinding of grain, etc. A French engineer, Benoit Fourneyron, developed the first commercially successful hydraulic turbine (circa 1830). Later Fourneyron built turbines for industrial purposes that achieved a speed of 2300 rev/min, developing about 50 kW at an efficiency of over 80%.

The American engineer James B. Francis designed the first *radial-inflow* hydraulic turbine that became widely used, gave excellent results, and was highly regarded. In its original form it was used for heads of between 10 and 100 m. A simplified form of this turbine is shown in Figure 1.1(d) in Chapter 1. It will be observed that the flow path followed is essentially from a radial direction to an axial direction.

The Pelton wheel turbine, named after its American inventor, Lester A. Pelton, was brought into use in the second half of the nineteenth century. This is an impulse turbine in which water is piped at high pressure to a nozzle where it expands completely to atmospheric pressure. The emerging jet impacts onto the blades (or buckets) of the turbine, which produce the required torque and power output. A simplified diagram of a Pelton wheel turbine is shown in Figure 1.1(f). The head of water used originally was between about 90 and 900 m (modern versions operate up to heads of nearly 2000 m).

The increasing need for more power during the early years of the twentieth century also led to the invention of a turbine suitable for small heads of water, i.e., 3 to 9 m, in river locations where a dam could be built. In 1913 Viktor Kaplan revealed his idea of the propeller (or Kaplan) turbine, see Figure 1.1(e), which acts like a ship's propeller but in reverse. At a later date Kaplan improved his turbine by means of swiveling blades, which improved the efficiency of the turbine appropriate to the available flow rate and head.

### Flow Regimes for Maximum Efficiency

The efficiency of a hydraulic turbine can be defined as the work developed by the rotor in unit time divided by the difference in hydraulic energy between inlet and outlet of the turbine in unit time. The

efficiencies of the three principal types of hydraulic turbine just mentioned are shown in Figure 9.1 as functions of the power specific speed,  $\Omega_{sp}$ . From eqn. (2.15b), this is

$$\Omega_{sp} = \frac{\Omega \sqrt{P/\rho}}{(gH_E)^{5/4}}, \tag{9.1}$$

where  $P$  is the power delivered by the shaft,  $\rho$  is the density of water,  $H_E$  is the effective head at turbine entry, and  $\Omega$  is the rotational speed in radians per second. It is remarkable that the efficiency of the multi-stage Pelton turbine has now reached 92.5% at  $\Omega_{sp} \cong 0.2$  and that the Francis turbine can achieve an efficiency of 95 to 96% at an  $\Omega_{sp} \cong 1.0$  to 2.0.

The  $\Omega_{sp}$  regimes of these turbine types are of considerable importance to the designer as they indicate the most suitable choice of machine for an application. In general, low specific speed machines correspond to low volume flow rates and high heads, whereas high specific speed machines correspond to high volume flow rates and low heads. Table 9.3 summarises the normal operating ranges for the specific speed, the effective head, the maximum power and best efficiency for each type of turbine.

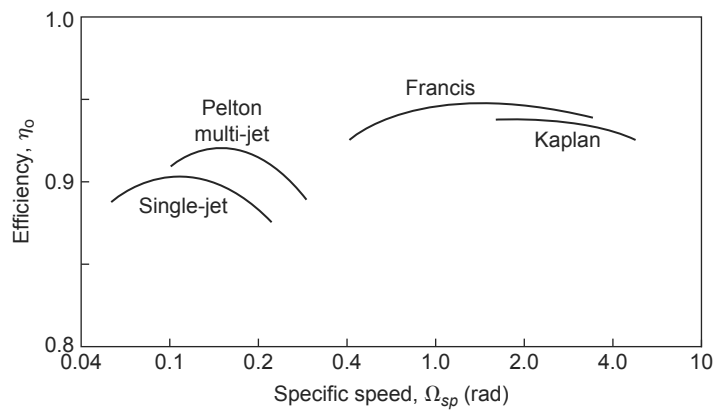


**FIGURE 9.1**  
Typical Design Point Efficiencies of Pelton, Francis, and Kaplan Turbines

<b>Table 9.3</b> Operating Ranges of Hydraulic Turbines			
	<b>Pelton Turbine</b>	<b>Francis Turbine</b>	<b>Kaplan Turbine</b>
Specific speed (rad)	0.05–0.4	0.4–2.2	1.8–5.0
Head (m)	100–1770	20–900	6–70
Maximum power (MW)	500	800	300
Optimum efficiency (%)	90	95	94
Regulation method	Needle valve and deflector plate	Stagger angle of guide vanes	Stagger angle of rotor blades

*Note: Values shown in the table are only a rough guide and are subject to change.*

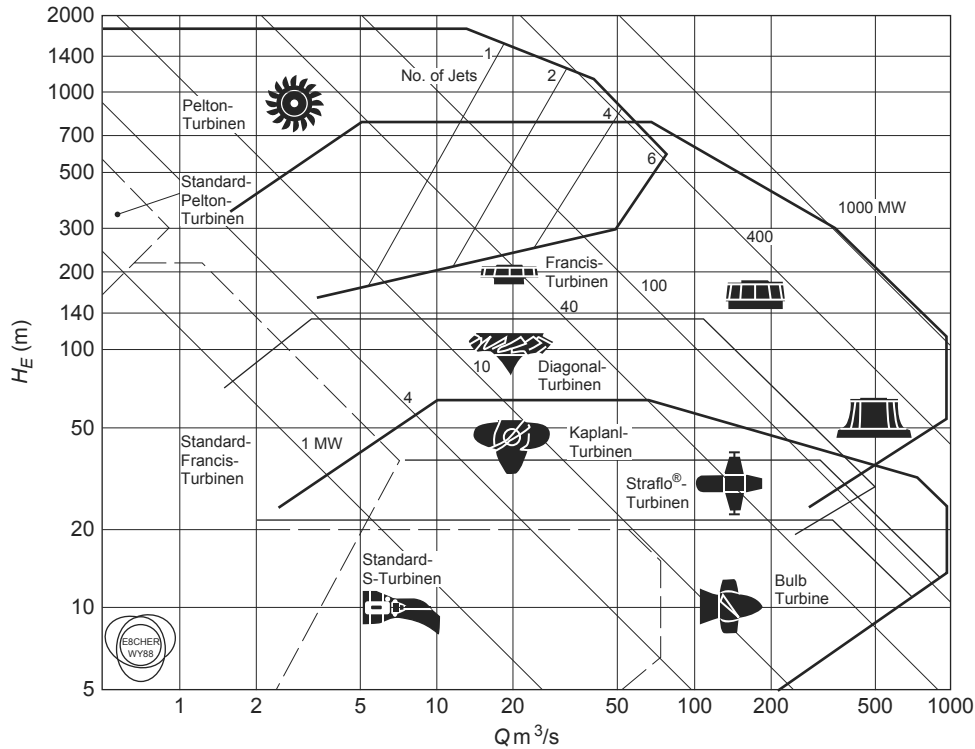


**FIGURE 9.2** Application Ranges for Various Types of Hydraulic Turbomachines, as a plot of  $Q$  versus  $H$  with Lines of Constant Power Determined Assuming  $\eta_0 = 0.8$  (Courtesy Sulzer Hydro Ltd., Zurich)

According to the experience of Sulzer Hydro Ltd., of Zurich, the application ranges of the various types of turbines and turbine pumps (including some not mentioned here) are plotted in Figure 9.2 on a  $\ln Q$  versus  $\ln H_E$  diagram and reflect the present state of the art of hydraulic turbomachinery design. Also in Figure 9.2 lines of constant power output are conveniently shown and have been calculated as the product  $\eta\rho gQH_E$  where the efficiency  $\eta$  is given the value of 0.8 throughout the chart.

### Capacity of Large Francis Turbines

The size and capacity of some of the recently built Francis turbines is a source of wonder, they seem so enormous! The size and weight of the runners cause special problems getting them to the site, especially when rivers have to be crossed and the bridges are inadequate.

The largest installation in North America (circa 1998) is at La Grande on James Bay in eastern Canada where 22 units each rated at 333 MW have a total capacity of 7326 MW. A close competitor with the Three Gorges project is the Itaipu hydroelectric plant on the Paraná river (between Brazil and Paraguay), which has a capacity of 12,600 MW in full operation using 18 Francis turbines each sized at 700 MW.

The efficiency of large Francis turbines has gradually risen over the years and now is about 95%. There seems to be little prospect of much further improvement in efficiency as computable values of losses due to skin friction, tip leakage, and exit kinetic energy from the diffuser are reckoned to account for the remaining 5%. Raabe (1985) has given much attention to the statistics of the world's biggest turbines. It would appear at the present time that the largest hydroturbines in the world are the three vertical shaft Francis turbines installed at Grand Coulee III on the Columbia River, Washington, United States. Each of these leviathans has been uprated to 800 MW, with the delivery (or effective) head,  $H_E = 87$  m,  $N = 85.7$  rev/min, the runner having a diameter of  $D = 9.26$  m and weighing 450 ton. Using this data in eqn. (9.1) it is easy to calculate that the power specific speed  $\Omega_{sp} = 1.74$  rad.

### 9.3 THE PELTON TURBINE

This is the only hydraulic turbine of the impulse type now in common use. It is an efficient machine and it is particularly suited to high head applications. The rotor consists of a circular disc with a number of blades (usually called *buckets*) spaced around the periphery. One or more nozzles are mounted in such a way that each nozzle directs its jet along a tangent to the circle through the centres of the buckets. A "splitter" or ridge splits the oncoming jet into two equal streams so that, after flowing round the inner surface of the bucket, the two streams depart from the bucket in a direction nearly opposite to that of the incoming jet.

Figure 9.3 shows the runner of a Pelton turbine and Figure 9.4 shows a six-jet vertical axis Pelton turbine. Considering one jet impinging on a bucket, the appropriate velocity diagram is shown in Figure 9.5. The jet velocity at entry is  $c_1$  and the blade speed is  $U$  so that the relative velocity at entry is  $w_1 = c_1 - U$ . At exit from the bucket one half of the jet stream flows as shown in the velocity diagram, leaving with a relative velocity  $w_2$  and at an angle  $\beta_2$  to the original direction of flow. From the velocity diagram the much smaller absolute exit velocity  $c_2$  can be determined.

From Euler's turbine equation, eqn. (1.18c), the specific work done by the water is

$$\Delta W = U_1 c_{\theta 1} - U_2 c_{\theta 2}.$$

For the Pelton turbine,  $U_1 = U_2 = U$ ,  $c_{\theta 1} = c_1$  so we get

$$\Delta W = U[U + w_1 - (U + w_2 \cos \beta_2)] = U(w_1 - w_2 \cos \beta_2),$$

in which the value of  $c_{\theta 2} < 0$ , as defined in Figure 9.5, i.e.,  $c_{\theta 2} = U + w_2 \cos \beta_2$ .

The effect of friction on the fluid flowing inside the bucket will cause the relative velocity at outlet to be less than the value at inlet. Writing  $w_2 = kw_1$ , where  $k < 1$ ,

$$\Delta W = Uw_1(1 - k \cos \beta_2) = U(c_1 - U)(1 - k \cos \beta_2). \quad (9.2)$$

An efficiency  $\eta_R$  for the runner can be defined as the specific work done  $\Delta W$  divided by the incoming kinetic energy, i.e.,

$$\eta_R = \Delta W / \left( \frac{1}{2} c_1^2 \right) = 2U(c_1 - U)(1 - k \cos \beta_2) / c_1^2. \quad (9.3)$$

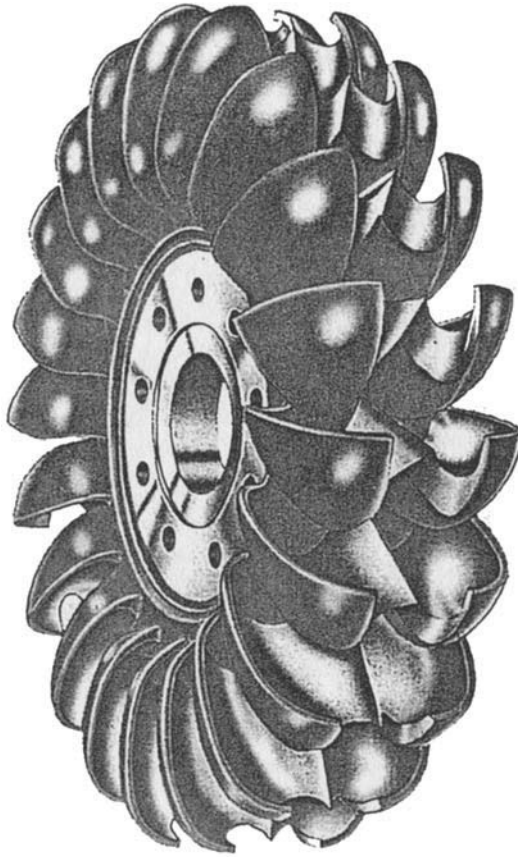


**FIGURE 9.3**  
Pelton Turbine Runner (Courtesy Sulzer Hydro Ltd., Zurich)

Therefore,

$$\eta_R = 2v(1-v)(1-k \cos \beta_2), \quad (9.4)$$

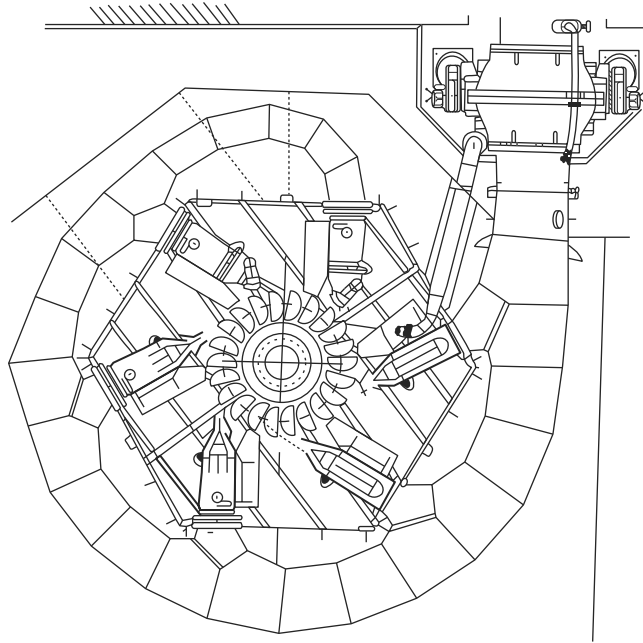
where the blade speed to jet speed ratio,  $v = U/c_1$ .

To find the optimum efficiency, differentiate eqn. (9.4) with respect to the blade speed ratio, i.e.,

$$\frac{d\eta_R}{dv} = 2 \frac{d}{dv} (v - v^2)(1 - k \cos \beta_2) = 2(1 - 2v)(1 - k \cos \beta_2) = 0.$$

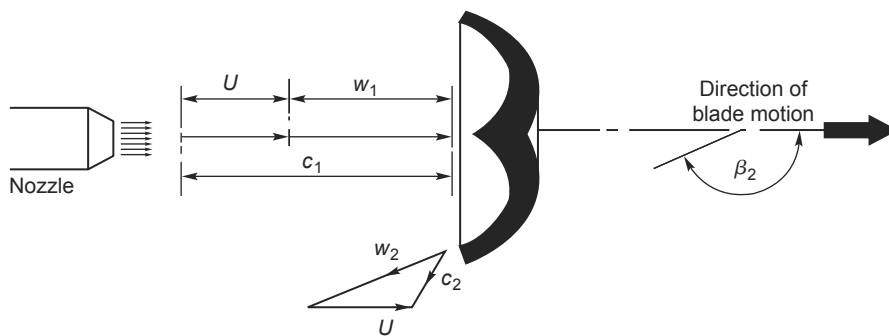
Therefore, the maximum efficiency of the runner occurs when  $v = 0.5$ , i.e.,  $U = c_1/2$ . Hence,

$$\eta_{R \max} = (1 - k \cos \beta_2). \quad (9.5)$$



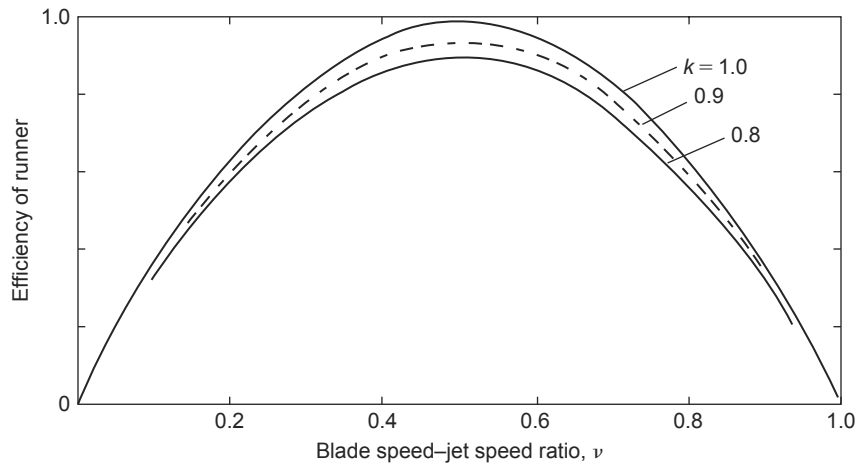
**FIGURE 9.4**

Six-Jet Vertical Shaft Pelton Turbine, Horizontal Section; Power Rating 174.4 MW, Runner Diameter 4.1 m, Speed 300 rev/min, Head 587 m (Courtesy Sulzer Hydro Ltd., Zurich)



**FIGURE 9.5**

The Pelton Wheel Showing the Jet Impinging onto a Bucket and the Relative and Absolute Velocities of the Flow (Only One Half of the Emergent Velocity Diagram Is Shown)

**FIGURE 9.6**

Theoretical Variation of Runner Efficiency for a Pelton Wheel with a Blade Speed–Jet Speed Ratio for several Values of Friction Factor  $k$

Figure 9.6 shows the theoretical variation of the runner efficiency with blade speed ratio for assumed values of  $k = 0.8, 0.9,$  and  $1.0$  with  $\beta_2 = 165^\circ$ . In practice the value of  $k$  is usually found to be between  $0.8$  and  $0.9$ .

### A Simple Hydroelectric Scheme

The layout of a Pelton turbine hydroelectric scheme is shown in Figure 9.7. The water is delivered from a constant level reservoir at an elevation  $z_R$  (above sea level) and flows via a pressure tunnel to the penstock head, down the penstock to the turbine nozzles emerging onto the buckets as a high speed jet. To reduce the deleterious effects of large pressure surges, a *surge tank* is connected to the flow close to the penstock head, which acts so as to damp out transients. The elevation of the nozzles is  $z_N$  and the gross head,  $H_G = z_R - z_N$ .

### Controlling the Speed of the Pelton Turbine

The Pelton turbine is usually directly coupled to an electrical generator that must run at synchronous speed. With large size hydroelectric schemes supplying electricity to a national grid it is essential for both the voltage and the frequency to closely match the grid values. To ensure that the turbine runs at constant speed despite any load changes that may occur, the rate of flow  $Q$  is changed. A spear (or needle) valve, Figure 9.8(a), whose position is controlled by means of a servomechanism, is moved axially within the nozzle to alter the diameter of the jet. This works well for very gradual changes in load. However, when a sudden loss in load occurs a more rapid response is needed. This is accomplished by temporarily deflecting the jet with a deflector plate so that some of the water does not reach the buckets, Figure 9.8(b). This acts to prevent over-speeding and allows time for the slower acting spear valve to move to a new position.

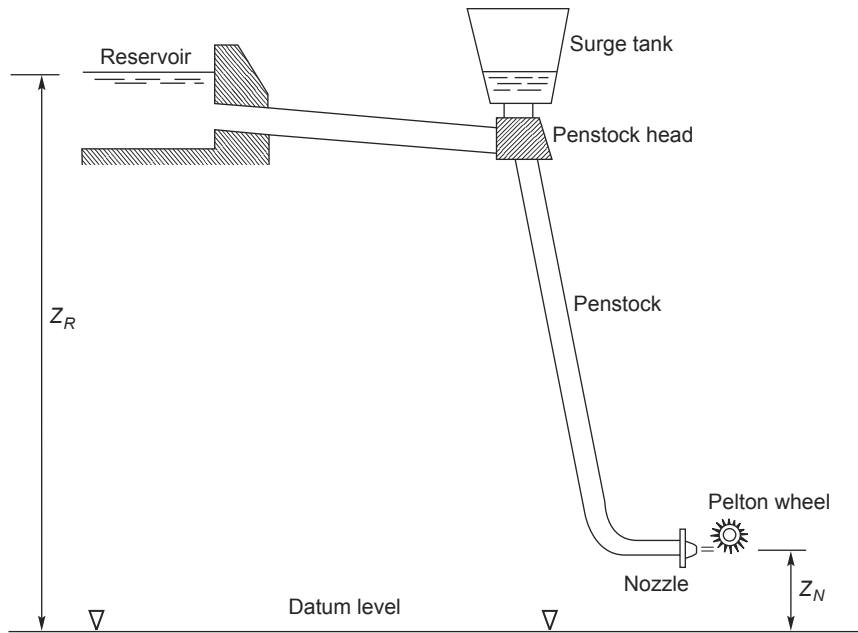


**FIGURE 9.7**  
Pelton Turbine Hydroelectric Scheme

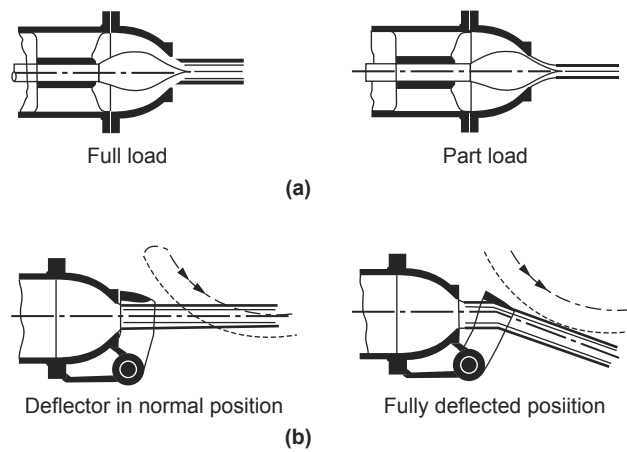


**FIGURE 9.8**  
Methods of Regulating the Speed of a Pelton Turbine: (a) with a Spear (or Needle) Valve; (b) with a Deflector Plate

It is vital to ensure that the spear valve *does move slowly* as a sudden reduction in the rate of flow could result in serious damage to the system from pressure surges (called *water hammer*). If the spear valve did close quickly, all the kinetic energy of the water in the penstock would be absorbed by the elasticity of the supply pipeline (penstock) and the water, creating very large stresses, which would reach their greatest intensity at the turbine inlet where the pipeline is already heavily stressed. The surge chamber, shown in Figure 9.7, has the function of absorbing and dissipating some of the pressure and energy fluctuations created by too rapid a closure of the needle valve.

### Sizing the Penstock

It is shown in elementary textbooks on fluid mechanics, e.g., Shames (1992) and Douglas, Gasiorek, and Swaffield (1995), that the loss in head with incompressible, steady, turbulent flow in pipes of circular cross-section is given by Darcy's equation:

$$H_f = \frac{2f l V^2}{g d}, \quad (9.6)$$

where  $f$  is the friction factor,  $l$  is the length of the pipe,  $d$  is the pipe diameter, and  $V$  is the mass average velocity of the flow in the pipe. It is assumed, of course, that the pipe is running full. The value of the friction factor has been determined for various conditions of flow and pipe surface roughness and the results are usually presented in what is called a *Moody diagram*. This diagram gives values of  $f$  as a function of pipe Reynolds number for varying levels of relative roughness of the pipe wall.

The penstock (the pipeline bringing the water to the turbine) is long and of large diameter and this can add significantly to the total cost of a hydroelectric power scheme. Using Darcy's equation it is easy to calculate a suitable pipe diameter for such a scheme if the friction factor is known and an estimate can be made of the allowable head loss. Logically, this head loss would be determined on the basis of the cost of materials etc., needed for a large diameter pipe and compared with the value of the useful energy lost from having too small a pipe. A commonly used compromise for the loss in head in the supply pipes is to allow  $H_f \leq 0.1 H_G$ .

From eqn. (9.6), substituting for the velocity,  $V = 4Q/(\pi d^2)$ , we get

$$H_f = \left( \frac{32 f l}{\pi^2 g} \right) \frac{Q^2}{d^5}. \quad (9.7)$$

#### EXAMPLE 9.1

Water is supplied to a turbine at the rate  $Q = 2.272 \text{ m}^3/\text{s}$  by a single penstock 300 m long. The allowable head loss due to friction in the pipe amounts to 20 m. Determine the diameter of the pipe if the friction factor  $f = 0.01$ .

#### Solution

Rearranging eqn. (9.7)

$$d^5 = \frac{32 f l}{g H_f} \left( \frac{Q}{\pi} \right)^2 = \frac{32 \times 0.01 \times 300}{9.81 \times 20} \left( \frac{2.272}{\pi} \right)^2 = 0.2559.$$

Therefore,  $d = 0.7614 \text{ m}$ .

### Energy Losses in the Pelton Turbine

Having accounted for the energy loss due to friction in the penstock, the energy losses in the rest of the hydroelectric scheme must now be considered. The effective head,  $H_E$  (or delivered head), at entry to the turbine is the gross head minus the friction head loss,  $H_f$ , i.e.,

$$H_E = H_G - H_f = z_R - z_N - H_f$$

and the spouting (or ideal) velocity,  $c_o$ , is

$$c_o = \sqrt{2gH_E}.$$

The pipeline friction loss  $H_f$  is regarded as an external loss and is not usually included in the losses attributed to the turbine itself. The performance and efficiency of the turbine are, in effect, measured against the total head,  $H_E$ , as shown in the following.

The main energy losses of the turbine occur in

- (i) the nozzles due to fluid friction;
- (ii) converting the kinetic energy of the jet into mechanical energy of the runner;
- (iii) external effects (bearing friction and windage).

Each of these energy losses are now considered in turn.

For *item (i)* let the loss in head in the nozzles be  $\Delta H_N$ . Thus, the available head is

$$H_E - \Delta H_N = c_1^2/(2g), \quad (9.8)$$

where  $c_1$  is the actual velocity of the jet at nozzle exit. The nozzle efficiency is defined by

$$\eta_N = \frac{\text{energy at nozzle exit}}{\text{energy at nozzle inlet}} = \frac{c_1^2}{2gH_E}. \quad (9.9a)$$

This efficiency is usually very close to 100% as the flow is accelerating through the nozzle. An often-used alternative to  $\eta_N$  is the nozzle velocity coefficient  $K_N$  defined by

$$K_N = \frac{\text{actual velocity at nozzle exit}}{\text{spouting velocity}} = \frac{c_1}{c_o},$$

i.e.,

$$\eta_N = K_N^2 = \frac{c_1^2}{c_o^2}. \quad (9.9b)$$

For *item (ii)* the loss in energy is already described in eqn. (9.2) and the runner efficiency  $\eta_R$  by eqns. (9.3) and (9.4). The turbine hydraulic efficiency  $\eta_h$  is defined as the specific work done by the rotor,  $\Delta W$ , divided by the specific energy available at entry to the nozzle,  $gH_E$ , i.e.,

$$\eta_h = \frac{\Delta W}{gH_E} = \left( \frac{\Delta W}{\frac{1}{2}c_1^2} \right) \left( \frac{\frac{1}{2}c_1^2}{gH_E} \right) = \eta_R \eta_N, \quad (9.10)$$

after using eqn. (9.9a).

For *item (iii)* the external losses are responsible for the energy deficit between the runner and the shaft. A good estimate of these losses can be made using the following simple flow model where the specific energy loss is assumed to be proportional to the square of the blade speed, i.e.,

$$\text{external loss/unit mass flow} = KU^2,$$

where  $K$  is a dimensionless constant of proportionality. Thus, the shaft work done/unit mass flow is

$$\Delta W - KU^2.$$

Therefore, the overall efficiency of the turbine,  $\eta_o$ , including these external losses is

$$\eta_o = (\Delta W - KU^2)/(gH_e),$$

i.e., the shaft work delivered by the turbine/specific energy available at nozzle entry, which

$$= \eta_R \eta_N - 2K \left(\frac{U}{c_1}\right)^2 \left(\frac{c_1^2}{2gH_E}\right).$$

Using the definitions of the blade speed–jet speed ratio,  $v = U/c_1$ , and the nozzle efficiency,  $\eta_N = c_1^2/c_2^2$ ,

$$\eta_o = \eta_N(\eta_R - 2Kv^2) = \eta_m \eta_R \eta_N, \tag{9.11}$$

where the mechanical efficiency,  $\eta_m = 1 - \text{external losses}/gH_E$ , i.e.,

$$\eta_m = 1 - 2Kv^2/\eta_R. \tag{9.12}$$

The variation of the overall efficiency as given by eqn. (9.11) is shown in Figure 9.9 as a function of  $v$  for several values of the windage coefficient  $K$ . It will be noticed that peak efficiency reduces as the value of  $K$  is increased and that it occurs at lower values of  $v$  than the optimum for the runner. This evaluation of the theoretical performance of a Pelton turbine gives a possible reason for the often puzzling result given when experiments are evaluated and that always yield a peak efficiency for values of  $v < 0.5$ .

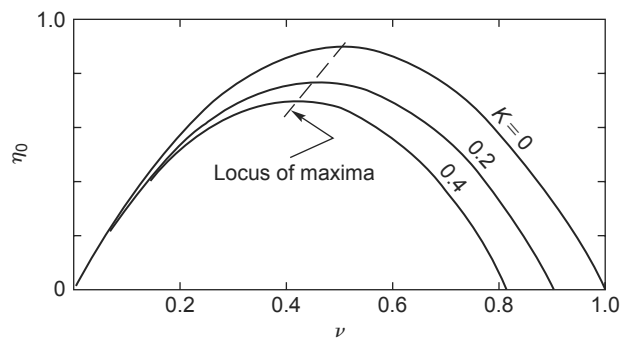


**FIGURE 9.9** Variation of Overall Efficiency of a Pelton Turbine with Speed Ratio for Several Values of Windage Coefficient,  $K$

By differentiating eqn. (9.11) it can be shown that the optimum value of  $v$  occurs when

$$v_{\text{opt}} = \frac{A}{2(A + K)}.$$

where  $A = 1 - k \cos \beta_2$ .

### Exercise

Let  $k = 0.9$ ,  $\beta_2 = 165^\circ$ , and  $K = 0.1$ . Hence,  $A = 1.869$  and  $v = 0.475$ .

Typical performance of a Pelton turbine *under conditions of constant head and speed* is shown in Figure 9.10 in the form of the variation of overall efficiency against load ratio. As a result of a change in the load the output of the turbine must then be regulated by a change in the setting of the needle valve to keep the turbine speed constant. The observed almost constant value of the efficiency over most of the load range is the result of the *hydraulic losses* reducing in proportion to the power output. However, as the load ratio is reduced to even lower values, the windage and bearing friction losses, which have not diminished, assume a relatively greater importance and the overall efficiency rapidly diminishes towards zero.

### EXAMPLE 9.2

A Pelton turbine is driven by two jets, generating 4.0 MW at 375 rev/min. The effective head at the nozzles is 200 m of water and the nozzle velocity coefficient,  $K_N = 0.98$ . The axes of the jets are tangent to a circle 1.5 m in diameter. The relative velocity of the flow across the buckets is decreased by 15% and the water is deflected through an angle of  $165^\circ$ .

Neglecting bearing and windage losses, determine

- (i) the runner efficiency;
- (ii) the diameter of each jet;
- (iii) the power specific speed.

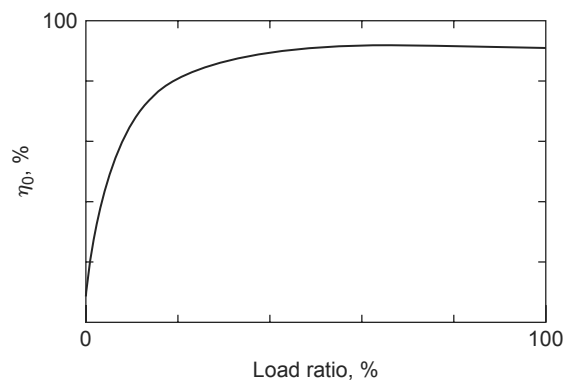


FIGURE 9.10

Pelton Turbine Overall Efficiency Variation with Load Under Constant Head and Constant Speed Conditions

**Solution**

- (i) The blade speed is

$$U = \Omega r = (375 \times \pi/30) \times 1.5/2 = 39.27 \times 1.5/2 = 29.45 \text{ m/s.}$$

The jet speed is

$$c_1 = K_N \sqrt{2gH_E} = 0.98 \times \sqrt{2 \times 9.81 \times 200} = 61.39 \text{ m/s.}$$

Therefore,  $v = U/c_1 = 0.4798$ .

The efficiency of the runner is obtained from eqn. (9.4):

$$\eta_R = 2 \times 0.4798 \times (1 - 0.4798)(1 - 0.85 \times \cos 165^\circ) = 0.9090.$$

- (ii) The “theoretical” power is
- $P_{th} = P/\eta_R = 4.0/0.909 = 4.40 \text{ MW}$
- , where
- $P_{th} = \rho g Q H_E$
- . Therefore,

$$Q = P_{th}/(\rho g H_E) = 4.4 \times 10^6 / (9810 \times 200) = 2.243 \text{ m}^3/\text{s.}$$

Each jet must have a flow area of

$$A_j = \frac{Q}{2c_1} = 2.243 / (2 \times 61.39) = 0.01827 \text{ m}^2.$$

Therefore,  $d_j = 0.5125 \text{ m}$ .

- (iii) Substituting into eqn. (9.1), the power specific speed is

$$\Omega_{sp} = 39.27 \times \left( \frac{4.0 \times 10^6}{10^3} \right)^{\frac{1}{3}} / (9.81 \times 200)^{\frac{5}{4}} = 0.190 \text{ rad.}$$

**9.4 REACTION TURBINES**

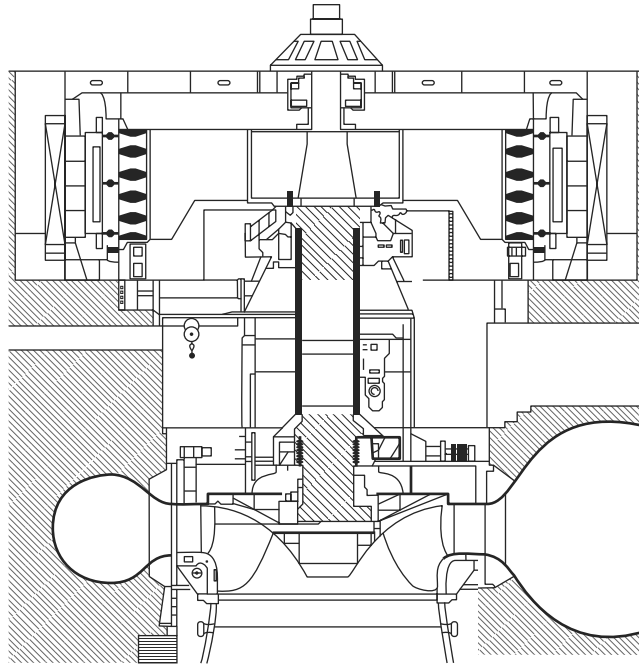
The primary features of the reaction turbine are

- (i) only part of the overall pressure drop has occurred up to turbine entry, the remaining pressure drop takes place in the turbine itself;
- (ii) the flow completely fills all of the passages in the runner, unlike the Pelton turbine where, for each jet, only one or two of the buckets at a time are in contact with the water;
- (iii) pivotable guide vanes are used to control and direct the flow;
- (iv) a draft tube is normally added on to the turbine exit; this is considered as an integral part of the turbine.

The pressure of the water gradually decreases as it flows through the runner and the reaction from this pressure change earns this type of turbine its appellation.

**9.5 THE FRANCIS TURBINE**

The majority of Francis turbines are arranged so that the axis is vertical (some smaller machines can have horizontal axes). Figure 9.11 illustrates a section through a vertical shaft Francis turbine with a runner diameter of 5 m, a head of 110 m, and a power rating of nearly 200 MW. Water enters via a

**FIGURE 9.11**

Vertical Shaft Francis Turbine: Runner Diameter 5 m, Head 110 m, Power 200 MW (Courtesy Sulzer Hydro Ltd., Zurich)

spiral casing called a *volute* or *scroll* that surrounds the runner. The area of cross-section of the volute decreases along the flow path in such a way that the flow velocity remains constant. From the volute the flow enters a ring of stationary guide vanes, which direct it onto the runner at the most appropriate angle.

In flowing through the runner the angular momentum of the water is reduced and work is supplied to the turbine shaft. At the design condition the absolute flow leaves the runner axially (although a small amount of swirl may be countenanced) into the *draft tube* and, finally, the flow enters the *tail-race*. It is essential that the exit of the draft tube is submerged below the level of the water in the tail-race in order that the turbine remains full of water. The draft tube also acts as a diffuser; by careful design it can ensure maximum recovery of energy through the turbine by significantly reducing the exit kinetic energy.

Figure 9.12 shows the runner of a small Francis turbine and Figure 9.13 is a sectional view of the turbine together with the velocity triangles at inlet to and exit from the runner at mid-blade height. At inlet to the guide vanes the flow is in the radial/tangential plane, the absolute velocity is  $c_1$  and the absolute flow angle is  $\alpha_1$ . Thus,

$$\alpha_1 = \tan^{-1}(c_{\theta 1}/c_{r1}). \quad (9.13)$$

**FIGURE 9.12**

Runner of a Small Francis Turbine (Permission Granted to Copy Under the Terms of the GNU Free Documentation License)

The flow is turned to angle  $\alpha_2$  and velocity  $c_2$ , the absolute condition of the flow at entry to the runner. By vector subtraction the relative velocity at entry to the runner is found, i.e.,  $w_2 = c_2 - U_2$ . The relative flow angle  $\beta_2$  at inlet to the runner is defined as

$$\beta_2 = \tan^{-1}[(c_{\theta 2} - U_2)/c_{r2}]. \quad (9.14)$$

Further inspection of the velocity diagrams in Figure 9.13 reveals that the direction of the velocity vectors approaching both guide vanes and runner blades are tangential to the camber lines at the leading edge of each row. This is the ideal flow condition for “shockless” low loss entry, although an incidence of a few degrees may be beneficial to output without a significant extra loss penalty. At vane outlet some deviation from the blade outlet angle is to be expected (see Chapter 3). For these reasons, in all problems concerning the direction of flow, it is clear that the angle of the fluid flow is important and not the vane angle as is often quoted in other texts.

At outlet from the runner the flow plane is simplified as though it were actually in the radial/tangential plane. This simplification will not affect the subsequent analysis of the flow but it must be conceded that some component of velocity in the axial direction does exist at runner outlet.

The water leaves the runner with a relative flow angle  $\beta_3$  and a relative flow velocity  $w_3$ . The absolute velocity at runner exit is found by vector addition, i.e.,  $c_3 = w_3 + U_3$ . The relative flow angle,  $\beta_3$ , at runner exit is given by

$$\beta_3 = \tan^{-1}[(c_{\theta 3} + U_3)/c_{r3}]. \quad (9.15)$$

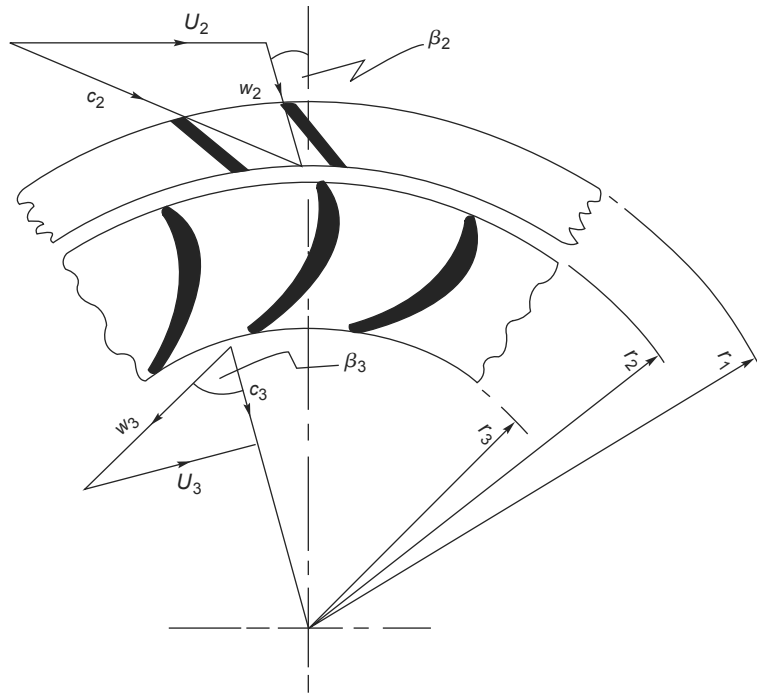


FIGURE 9.13

Sectional Sketch of Blading for a Francis Turbine Showing Velocity Diagrams at Runner Inlet and Exit

In this equation it is assumed that some residual swirl velocity  $c_{\theta 3}$  is present ( $c_{r3}$  is the radial velocity at exit from the runner). In most simple analyses of the Francis turbine it is assumed that there is no exit swirl. Detailed investigations have shown that some extra *counter-swirl* (i.e., acting so as to increase  $\Delta c_\theta$ ) at the runner exit does increase the amount of work done by the fluid without a significant reduction in turbine efficiency.

When a Francis turbine is required to operate at part load, the power output is reduced by swivelling the guide vanes to restrict the flow, i.e.,  $Q$  is reduced, while the blade speed is maintained constant. Figure 9.14 compares the velocity triangles at full load and at part load from which it will be seen that the relative flow at runner entry is at a high incidence and at runner exit the absolute flow has a large component of swirl. Both of these flow conditions give rise to high head losses. Figure 9.15 shows the variation of hydraulic efficiency for several types of turbine, including the Francis turbine, over the full load range at constant speed and constant head.

It is of interest to note the effect that swirling flow has on the performance of the following diffuser. The results of an extensive experimental investigation made by McDonald, Fox, and van Dewoestine (1971) showed that swirling inlet flow *does not* affect the performance of conical diffusers, which are well designed and give unseparated or only slightly separated flow when the flow through them is entirely axial. Accordingly, part load operation of the turbine is unlikely to give adverse diffuser performance.

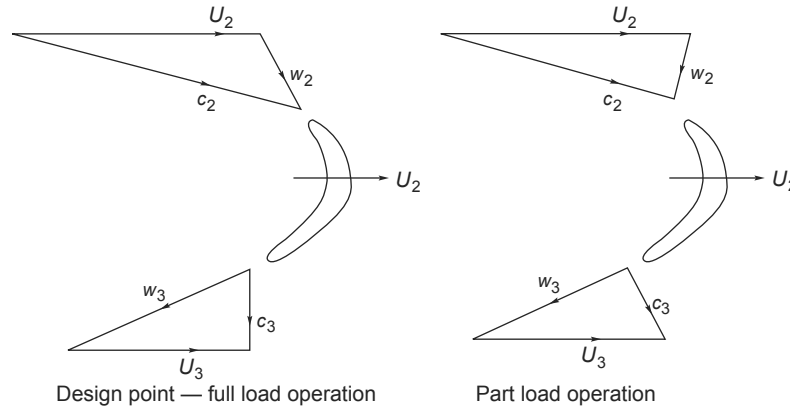


**FIGURE 9.14**  
Comparison of Velocity Triangles for a Francis Turbine at Full Load and at Part Load Operation

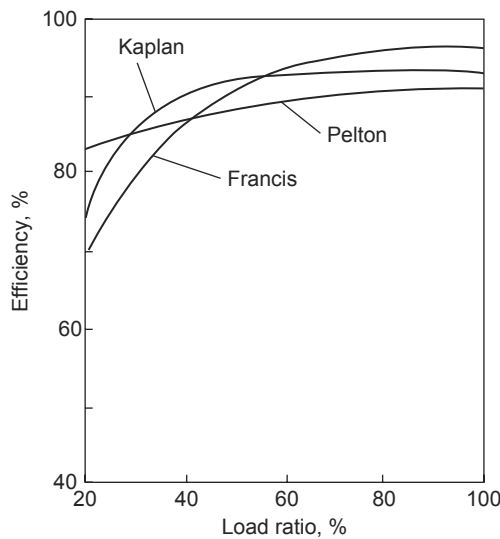


**FIGURE 9.15**  
Variation of Hydraulic Efficiency for Various Types of Turbine over a Range of Loading, at Constant Speed and Constant Head

**Basic Equations**

Euler’s turbine equation, eqn. (1.18c), in the present notation, is written as

$$\Delta W = U_2 c_{\theta 2} - U_3 c_{\theta 3}. \tag{9.16a}$$

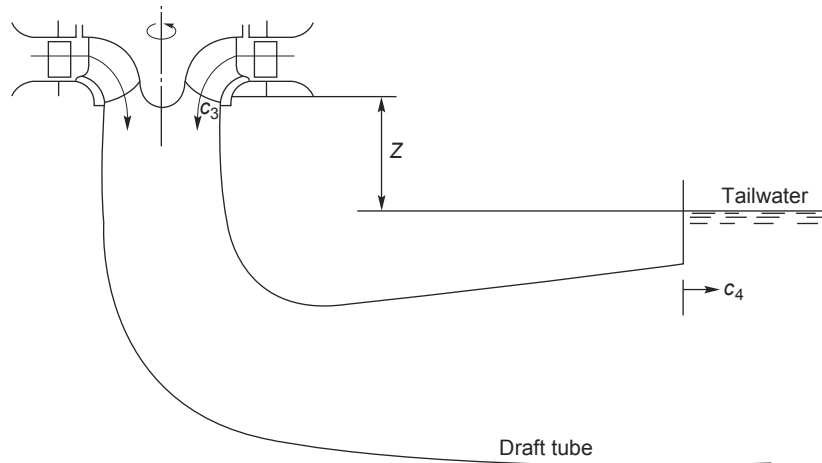


**FIGURE 9.16**  
Location of Draft Tube in Relation to Vertical Shaft Francis Turbine

If the flow at runner exit is without swirl then the equation reduces to

$$\Delta W = U_2 c_{\theta 2}. \quad (9.16b)$$

The effective head for all reaction turbines,  $H_E$ , is the total head available at the turbine inlet *relative to the surface of the tailrace*. At entry to the runner the energy available is equal to the sum of the kinetic, potential and pressure energies:

$$g(H_E - \Delta H_N) = \frac{p_2 - p_a}{\rho} + \frac{1}{2}c_2^2 + gz_2, \quad (9.17)$$

where  $\Delta H_N$  is the loss of head due to friction in the volute and guide vanes and  $p_2$  is the *absolute* static pressure at inlet to the runner.

At runner outlet the energy in the water is further reduced by the amount of specific work  $\Delta W$  and by friction work in the runner,  $g\Delta H_R$  and this remaining energy equals the sum of the pressure potential and kinetic energies:

$$g(H_E - \Delta H_N - \Delta H_R) - \Delta W = \frac{1}{2}c_3^2 + p_3/\rho - p_a/\rho + gz_3, \quad (9.18)$$

where  $p_3$  is the *absolute* static pressure at runner exit.

By differencing eqns. (9.17) and (9.18), the specific work is obtained:

$$\Delta W = (p_{02} - p_{03})/\rho - g\Delta H_R + g(z_2 - z_3), \quad (9.19)$$

where  $p_{02}$  and  $p_{03}$  are the absolute total pressures at runner inlet and exit.

Figure 9.16 shows the draft tube in relation to a vertical-shaft Francis turbine. The most important dimension in this diagram is the vertical distance ( $z = z_3$ ) between the exit plane of the runner and the

free surface of the tailrace. The energy equation between the exit of the runner and the tailrace can now be written as

$$p_3/\rho + \frac{1}{2}c_3^2 + gz_3 - g\Delta H_{DT} = \frac{1}{2}c_4^2 + p_a/\rho, \quad (9.20)$$

where  $\Delta H_{DT}$  is the loss in head in the draft tube and  $c_4$  is the flow exit velocity.

The hydraulic efficiency is defined by

$$\eta_h = \frac{\Delta W}{gH_E} = \frac{U_2c_{\theta 2} - U_3c_{\theta 3}}{gH_E} \quad (9.21a)$$

and, whenever  $c_{\theta 3} = 0$ ,

$$\eta_H = \frac{U_2c_{\theta 2}}{gH_E}. \quad (9.21b)$$

The overall efficiency is given by  $\eta_o = \eta_m\eta_H$ . For very large turbines (e.g., 500–1000 MW) the mechanical losses are then relatively small,  $\eta \rightarrow 100\%$  and effectively  $\eta_o \approx \eta_H$ .

For the Francis turbine the ratio of the runner tip speed to the jet velocity,  $v = U_2/c_1$ , is not as critical for high efficiency operation as it is for the Pelton turbine and can lie in a fairly wide range, e.g.,  $0.6 \leq v \leq 0.95$ . In most applications the Francis turbine is used to drive a synchronous generator and the rotational speeds chosen are those appropriate to either 50 or 60 cycles per second. The speed must then be maintained constant.

It is possible to obtain part load operation of the turbine by varying the angle of the guide vanes. The guide vanes are pivoted and set to an optimum angle via a gearing mechanism. However, part load operation normally causes a whirl velocity to be set up in the flow downstream of the runner causing a reduction in efficiency. The strength of the vortex may be enough to cause a cavitation bubble to form along the axis of the draft tube. (See Section 9.8, Cavitation.)

### EXAMPLE 9.3

In a vertical-shaft Francis turbine the available head at the inlet flange is 150 m of water and the vertical distance between the runner and the tailrace is 2.0 m. The runner tip speed is 35 m/s, the meridional velocity of the water through the runner is constant at 10.5 m/s, the flow leaves the runner without whirl and the velocity at exit from the draft tube is 3.5 m/s.

The hydraulic losses for the turbine are as follows:

$$\Delta H_N = 6.0 \text{ m}, \quad \Delta H_R = 10 \text{ m}, \quad \Delta H_{DT} = 1.0 \text{ m}.$$

Determine

- (i) the specific work,  $\Delta W$ , and the hydraulic efficiency,  $\eta_h$ , of the turbine;
- (ii) the absolute velocity,  $c_2$ , at runner entry;
- (iii) the pressure head (relative to the tailrace) at inlet to and exit from the runner;
- (iv) the absolute and relative flow angles at runner inlet;
- (v) if the flow discharged by the turbine is  $20 \text{ m}^3/\text{s}$  and the power specific speed is 0.8 (rad), the speed of rotation and diameter of the runner.

**Solution**

From eqns. (9.18) and (9.20), we can find the specific work,

$$\begin{aligned}\Delta W &= g(H_E - \Delta H_N - \Delta H_R - \Delta H_{DT}) - \frac{1}{2}c_4^2 \\ &= 9.81 \times (150 - 6 - 10 - 1) - 3.5^2/2 = 1298.6 \text{ m}^2/\text{s}^2.\end{aligned}$$

The hydraulic efficiency,  $\eta_h = \Delta W/(gH_E) = 0.8825$ .

As  $c_{\theta 3} = 0$ , then  $\Delta W = U_2 c_{\theta 2}$  and  $c_{\theta 2} = \Delta W/U_2 = 1298.6/35 = 37.1$  m/s, thus,

$$c_2 = \sqrt{c_{\theta 2}^2 + c_m^2} = \sqrt{37.1^2 + 10.5^2} = 38.56 \text{ m/s}.$$

From eqn. (9.17) the pressure head at inlet to the runner is

$$H_2 = H_E - \Delta H_N - c_2^2/(2g) = 150 - 6 - 38.56^2/(2 \times 9.81) = 68.22 \text{ m}.$$

Again, using eqn. (9.20), the pressure head (relative to the tailrace) at runner exit is

$$H_3 = (p_3 - p_a)/(\rho g) = (c_4^2 - c_3^2)/(2g) + \Delta H_{DT} - z_3 = (3.5^2 - 10.5^2)/(2 \times 9.81) + 1 - 2 = -6.0 \text{ m}.$$

Note: The minus sign for  $H_3$  indicates that the pressure is below the atmospheric level. This is a matter of considerable importance in the design and operation of hydraulic turbomachinery and is considered in further detail under the heading Cavitation later in this chapter.

The flow angles at runner inlet are now obtained as follows:

$$\alpha_2 = \tan^{-1}(c_{\theta 2}/c_{r2}) = \tan^{-1}(37.1/10.5) = 74.2^\circ$$

$$\beta_2 = \tan^{-1}[(c_{\theta 2} - U_2)/c_{r2}] = \tan^{-1}[(37.1 - 35)/10.5] = 11.31^\circ.$$

From the definition of power specific speed, eqn. (9.1), and using  $P/\rho = Q\Delta W$ ,

$$\Omega = \frac{\Omega_{SP}(gH_E)^{\frac{5}{4}}}{\sqrt{Q\Delta W}} = \frac{0.8 \times 9114}{\sqrt{20 \times 1298.7}} = 45.24 \text{ rad/s}.$$

Thus, the rotational speed  $N = 432$  rev/min and the runner diameter is

$$D_2 = 2U_2/\Omega = 70/45.24 = 1.547 \text{ m}.$$

## 9.6 THE KAPLAN TURBINE

This type of turbine evolved from the need to generate power from much lower pressure heads than are normally employed with the Francis turbine. To satisfy large power demands very large volume flow rates need to be accommodated in the Kaplan turbine, i.e., the product  $QH_E$  is large. The overall flow configuration is from radial to axial. Figure 9.17(a) is a part sectional view of a Kaplan turbine in which the flow enters from a volute into the inlet guide vanes, which impart a degree of swirl to